Supplementary Information

Colloid-like MXene/Phenolic Resin Composite Films with Multi-Interface Architectures for Enhanced Light-to-Heat Conversion.

Qing Zeng [a,b], *Mengxi Han* [a,b], *Jianlin Zhou* [a,b], *Yongjin Liu* [a], *Ruizheng Zhao* [c], *Xinhua Hu* [a*], *Bo You* [a,b*], *Limin Wu* [a,b]

[a] College of Smart Materials and Future Energy, Fudan University, Shanghai 200438, People's Republic of China

[b] State Key Laboratory of Coatings for Advanced Equipment, and Advanced Coatings Research Center of Ministry of Education, Fudan University, Shanghai 200438, People's Republic of China

[c] Engineering Research Center of Advanced Functional Material Manufacturing of Ministry of Education, School of Chemical Engineering, Zhengzhou University, Zhengzhou 450001, China.

E-mail: youbo@fudan.edu.cn (B. You), huxh@fudan.edu.cn (X. H. Hu)

1. Synthesis of Ti_3C_2 Nanosheets

Firstly, 1 g of lithium fluoride (LiF) was added into 20 mL of 9 mol/L hydrochloric acid (HCl) aqueous solution while stirring. Then, 1 g of titanium aluminum carbide (Ti_3AlC_2) was added into the above solution, and stirred at 40 °C for 48 h. After etching, the as-prepared product was washed with deionized water until the pH value was close to 6. The sediment was dispersed in deionized water, ultrasonicated for 2 h under nitrogen protection. Finally, the product was centrifugated at 4000 rad/min for 30 minutes and the supernatant was collected. The Ti_3C_2 powder was obtained after freeze drying.

2. Calculation

2.1 Theory

Eq. (1) was selected to determine the photothermal conversion efficiency.

$$\eta = \frac{\dot{\Phi}}{M \cdot S} \#(1)$$

Where η is photothermal efficiency, M(W m^{-2}) is irradiance, S(m^2) is the area of coatings perpendicular to the light, and $\dot{\Phi}$(J/m^3) is the heat released by inside heat source.

Eq. (2) was a differential equation of heat conduction in Cartesian coordinates, but since films and light had a cylindrical symmetry, a cylindrical coordinate was selected, and **Eq. (3)** was used.

$$\rho c\frac{\partial t}{\partial \tau} = \frac{\partial}{\partial x}\left(\lambda\frac{\partial t}{\partial x}\right) + \frac{\partial}{\partial y}\left(\lambda\frac{\partial t}{\partial y}\right) + \frac{\partial}{\partial z}\left(\lambda\frac{\partial t}{\partial z}\right) + \dot{\Phi} \#(2)$$

$$\rho c\frac{\partial t}{\partial \tau} = \frac{1}{r}\frac{\partial}{\partial r}\left(\lambda r\frac{\partial t}{\partial r}\right) + \frac{\partial}{\partial z}\left(\lambda\frac{\partial t}{\partial z}\right) + \dot{\Phi} \#(3)$$

Where c(J K^{-1}) is heat capacity, t(K) is temperature of films, τ(s) is time, λ(W m^{-1} K^{-1}) is heat conductivity, and ρ(kg m^{-3}) is density of films.

According to the measure environment, and the smooth surface of the films, the boundary presented as **Eq. (4)** and **Eq. (5)**, and the condition was natural convection in an infinite space.

$$-\lambda\left(\frac{\partial t}{\partial r}\right)_w = h(t_w - t_f) \#(4)$$

$$-\lambda\left(\frac{\partial t}{\partial z}\right)_w = h(t_w - t_f) \#(5)$$

Where t_w(K) is surface temperature of films, t_f(K) is air temperature, and h(W K^{-1} m^{-2}) is surface heat transfer coefficient.

If the temperature distribution could be measured, $\dot{\Phi}$ would be obtained. However, it was almost impossible to measure the temperature distribution in our

current experimental conditions. Therefore, $\dot{\Phi}$ should be simplified to be a simple form, so that it can be calculated with limited data. Since the thickness of the film is very small (less than 50 μm), and the thermal conductivity is relatively large (0.2~0.3 for polymer materials), so $\dot{\Phi}$ could be perceived as a constant in the z direction, and its distribution in the r direction is determined by the irradiance distribution on the surface (**Eq. (6)** for simulated solar light, **Eq. (7)** and **Eq. (8)** for laser).

$$\dot{\Phi} = a \#(6)$$

$$\frac{\partial \dot{\Phi}}{\partial z} = \frac{\partial \dot{\Phi}}{\partial \varphi} = 0 \#(7)$$

$$\frac{\partial \dot{\Phi}}{\partial r} = Qe^{\left(-2\frac{r^2}{R^2}\right)} \#(8)$$

Where a(W m^{-3}) is density of power of heat source, Q(W) is total heat produced by inside heat source, and R(m) is radius of light spot.

2.2 Modeling

Comsol 5.4, a FEA software, was chosen to calculate the photothermal conversion efficiency of the MXene/ phenolic colloid-like films, and to check the accuracy of the photothermal experiment.

For the laser source, a 10 mm radius disc with a thickness corresponding to a particular sample was constructed, and a coaxial 1.5 mm was selected as the light absorbing area (**Figure S1**). A Gaussian distribution heat flux in the r direction (described by **Eq. (8)**) was designed to be the only heat source. The heat transfer took place under the condition of natural thermal convection in infinite space. And the average temperature of a central circular area with a radius of 0.5 mm in the light absorbing field at different times was calculated to compare with the experimental result (**Figures S4 and S5**).

In contrast to the laser light source, a disc with a radius of 5 mm and a thickness corresponding to a specific sample was constructed for the simulated solar light source (**Figure S2**). Because the temperature field of the disc fluctuated, the average temperature of a 1 mm-radius disc was chosen to match the temperature that was measured by an infrared thermal imager in the experiment (**Figures S6 and S7**). A constant heat flux was established throughout the disc. The heat transfer condition was the same as above. The parameters of different films in the calculation were represented in **Table S1**.

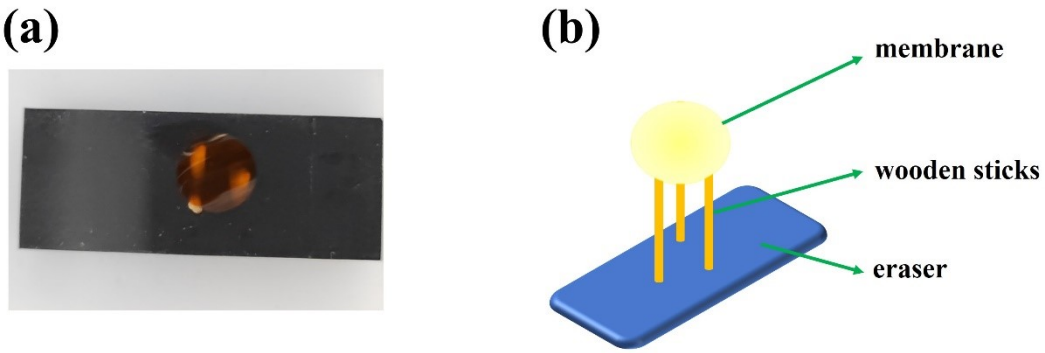

Figure S1. (a) Photograph of the device used in photo thermal test of film under simulated sunlight. (b) Schematic illustration of the device used in photo thermal test of film under simulated solar light.

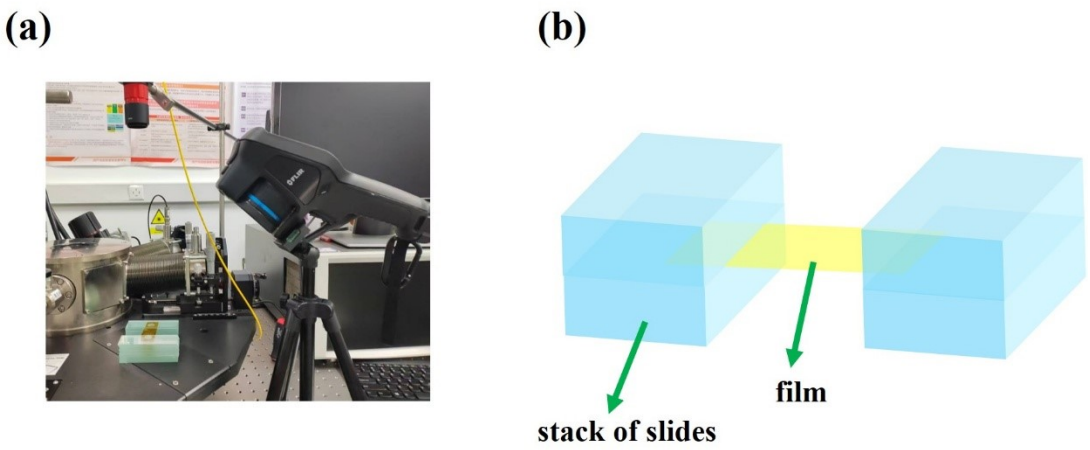

Figure S2. (a) Photograph of the device used in photo thermal test of film under 850 nm laser. (b) Schematic illustration of the device used in photo thermal test of film under 850 nm laser.

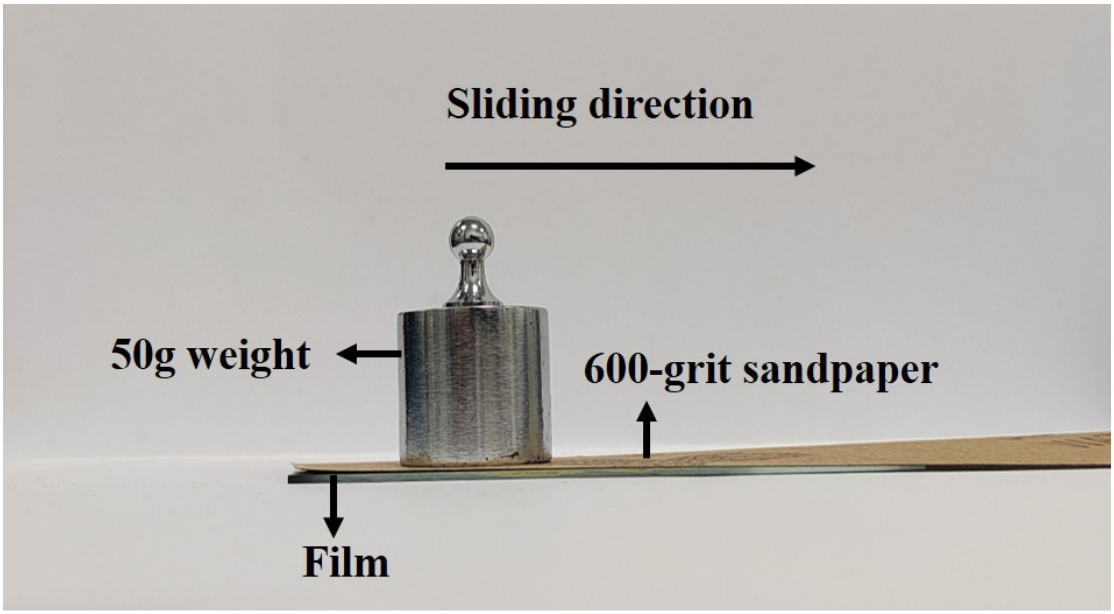

Figure S3. Schematic illustration of the friction test setup used to evaluate the wear resistance of the films.

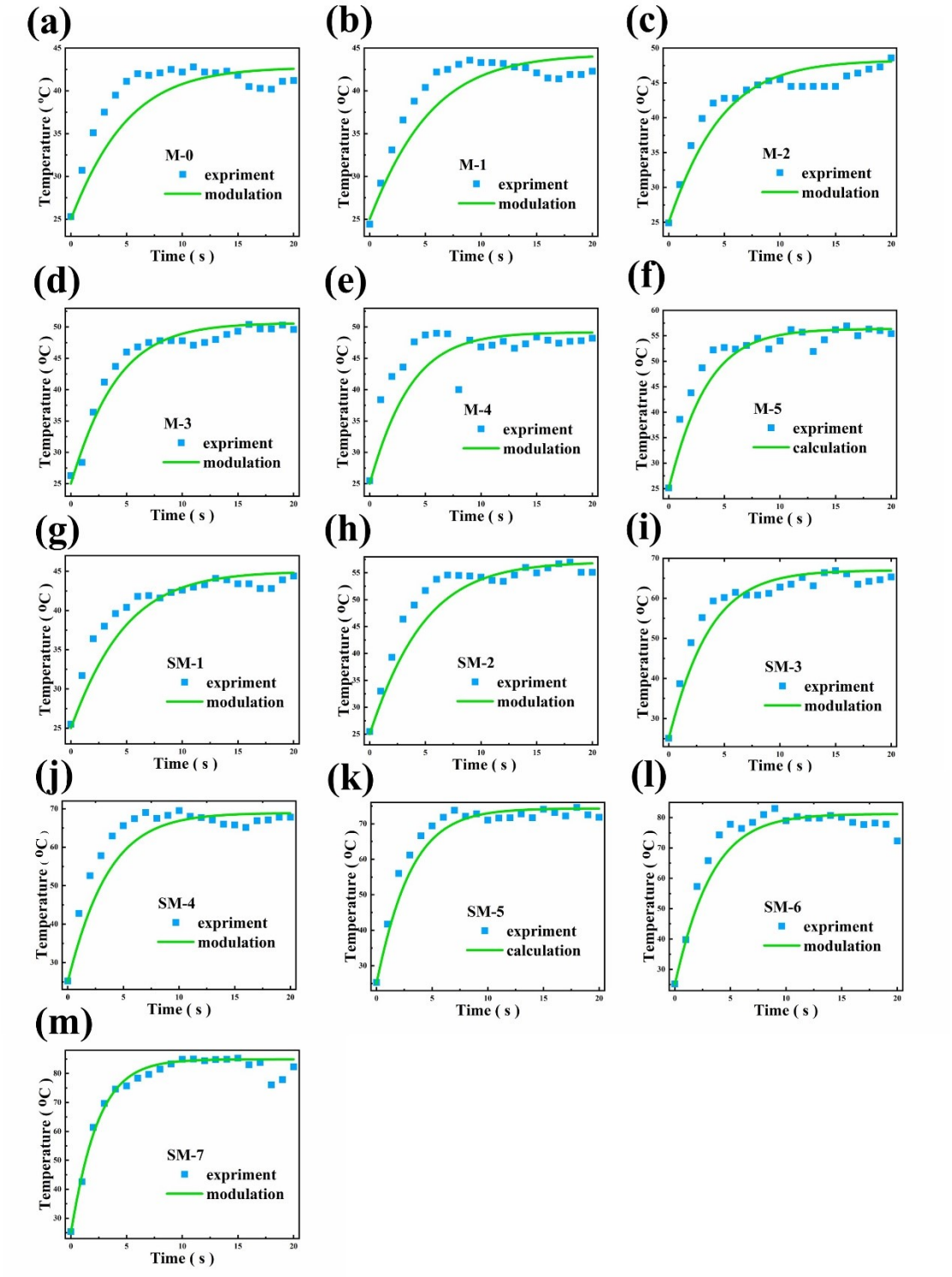

Figure S4. Curves of temperature change under simulated solar light irradiation in experiment and calculation of different films.

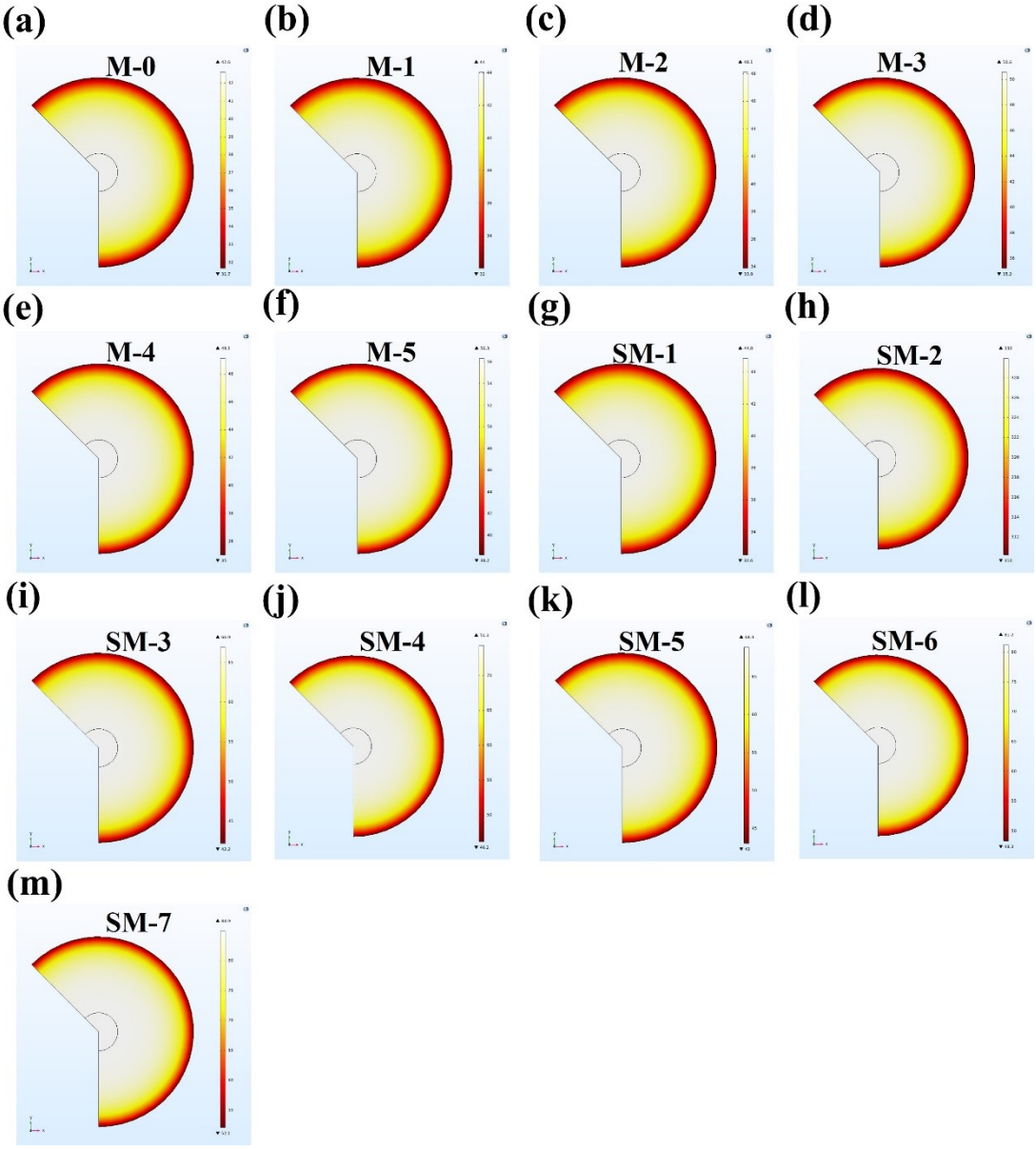

Figure S5. Surface temperature distribution of different films after heating for 20 s under simulated solar light irradiation in calculation.

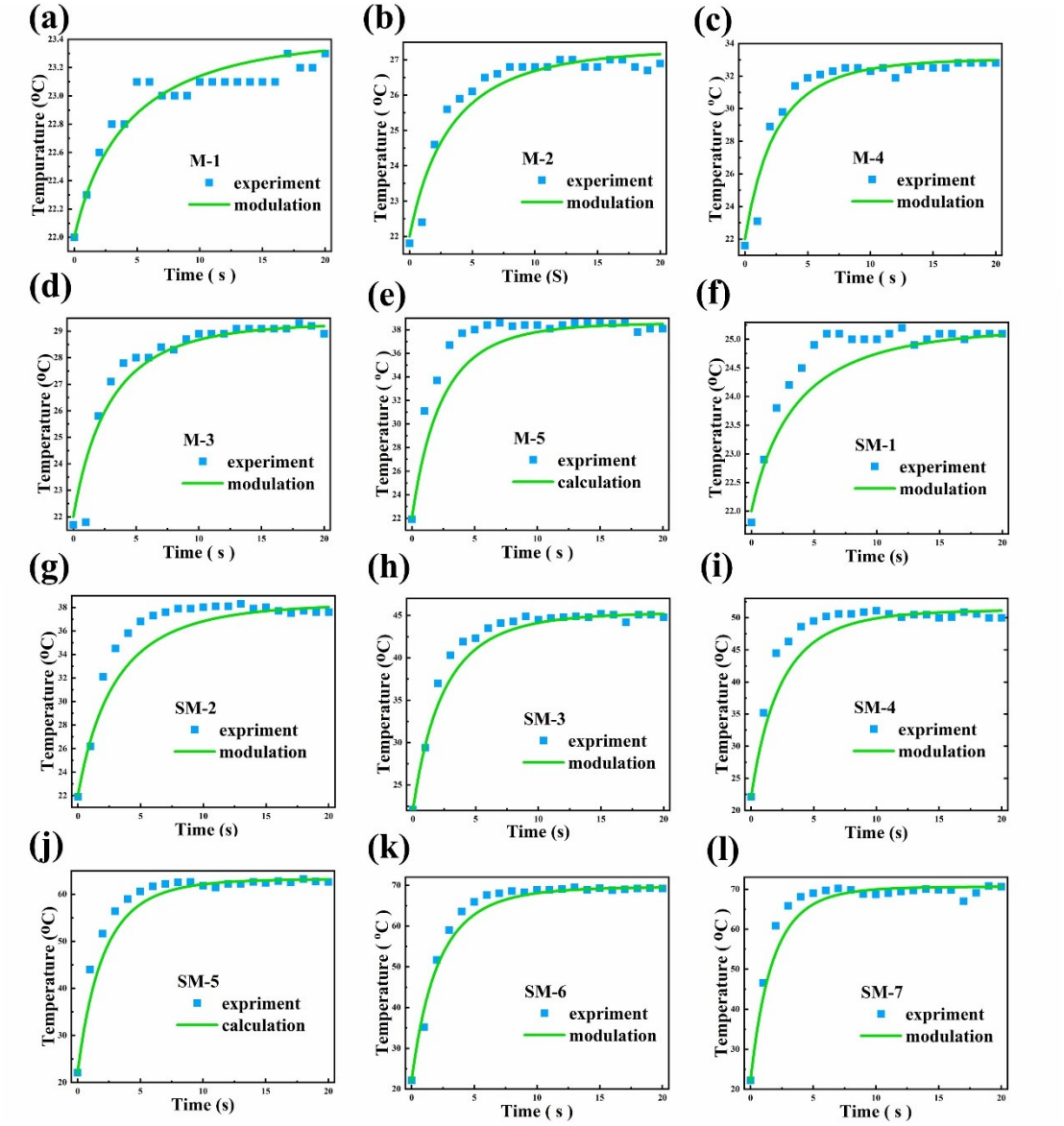

Figure S6. Curves of temperature change under 850nm laser irradiation in experiment and calculation of different films.

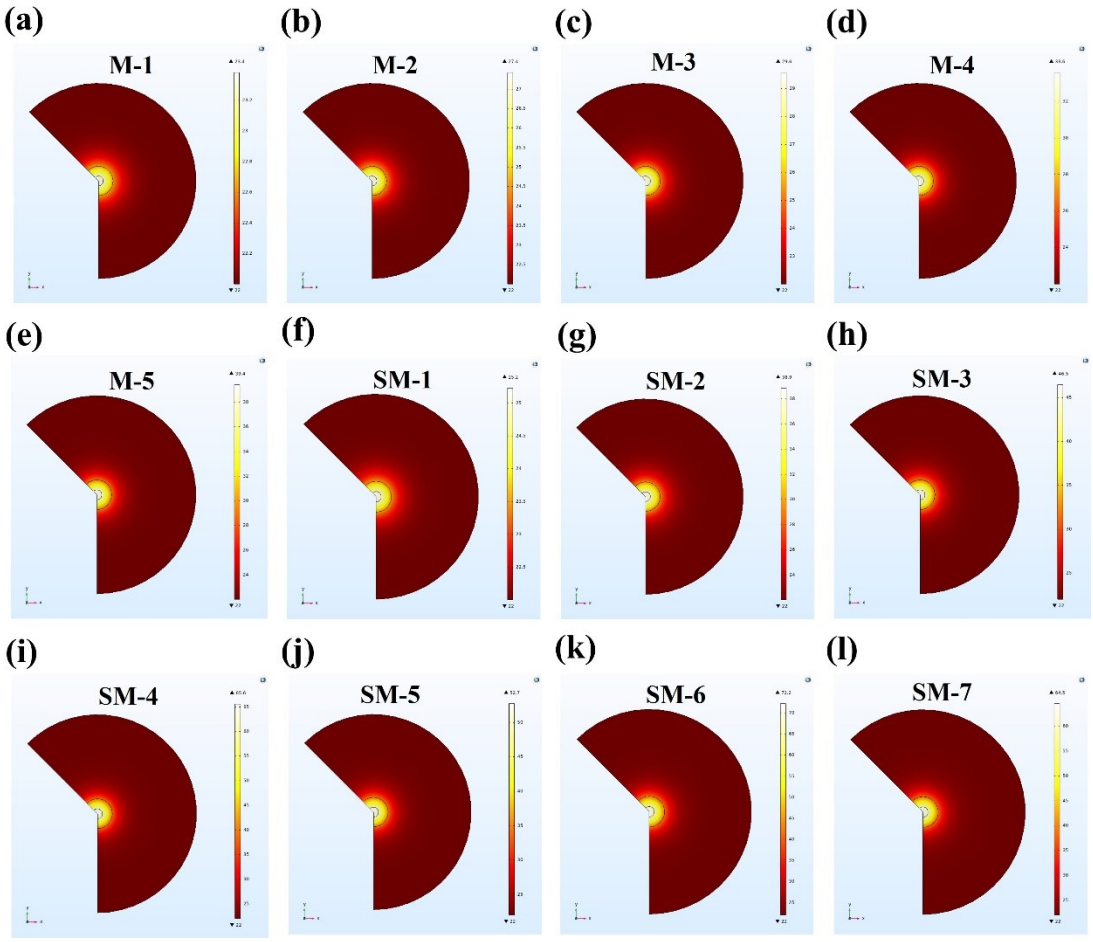

Figure S7. Surface temperature distribution of different films after heating for 20 s under laser irradiation in calculation.

Table S1. Parameters used in photothermal calculation.

Sample	M-0	M-1	M-2	M-3	M-4	M-5	SM-1	SM-2	SM-3	SM-4	SM-5	SM-6	SM-7
c (J/Kg·°C) (obtained in DSC)	1.43	-	-	1.52	-	1.52	-	-	1.49	-	1.42	1.36	1.37
c (J/Kg·°C) (used in calculation)	1.40	1.40	1.40	1.50	1.50	1.50	1.50	1.50	1.50	1.40	1.40	1.35	1.35
Thickness of film (μm)	45	50	45	40	35	35	45	50	40	35	40	40	30
ρ (kg/m^3)	1300	1300	1300	1300	1300	1300	1300	1300	1300	1300	1300	1400	1400
λ(W/(m · K)	0.3	0.3	0.3	0.3	0.3	0.3	0.3	0.3	0.3	0.3	0.3	0.3	0.3

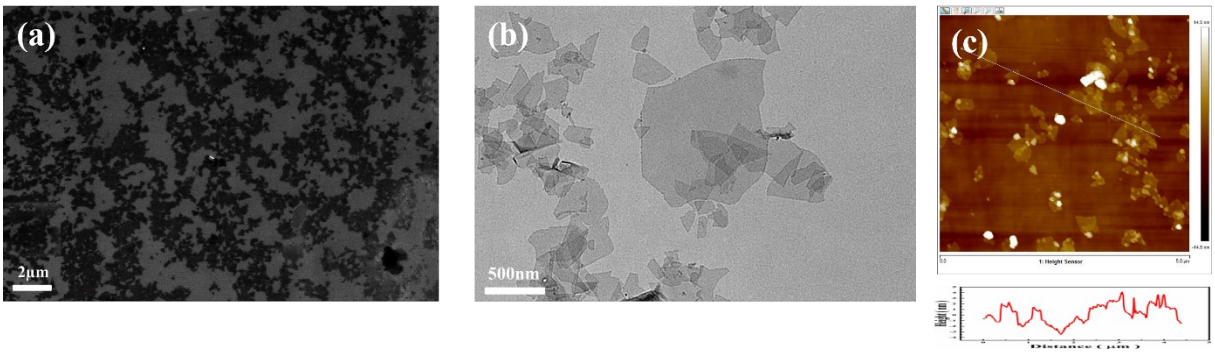

Figure S8. (a) SEM image of unmodified MXene nanoflakes. (b)TEM image of unmodified MXerne nanoflakes. (c) AFM image of unmodified MXene nanoflakes.

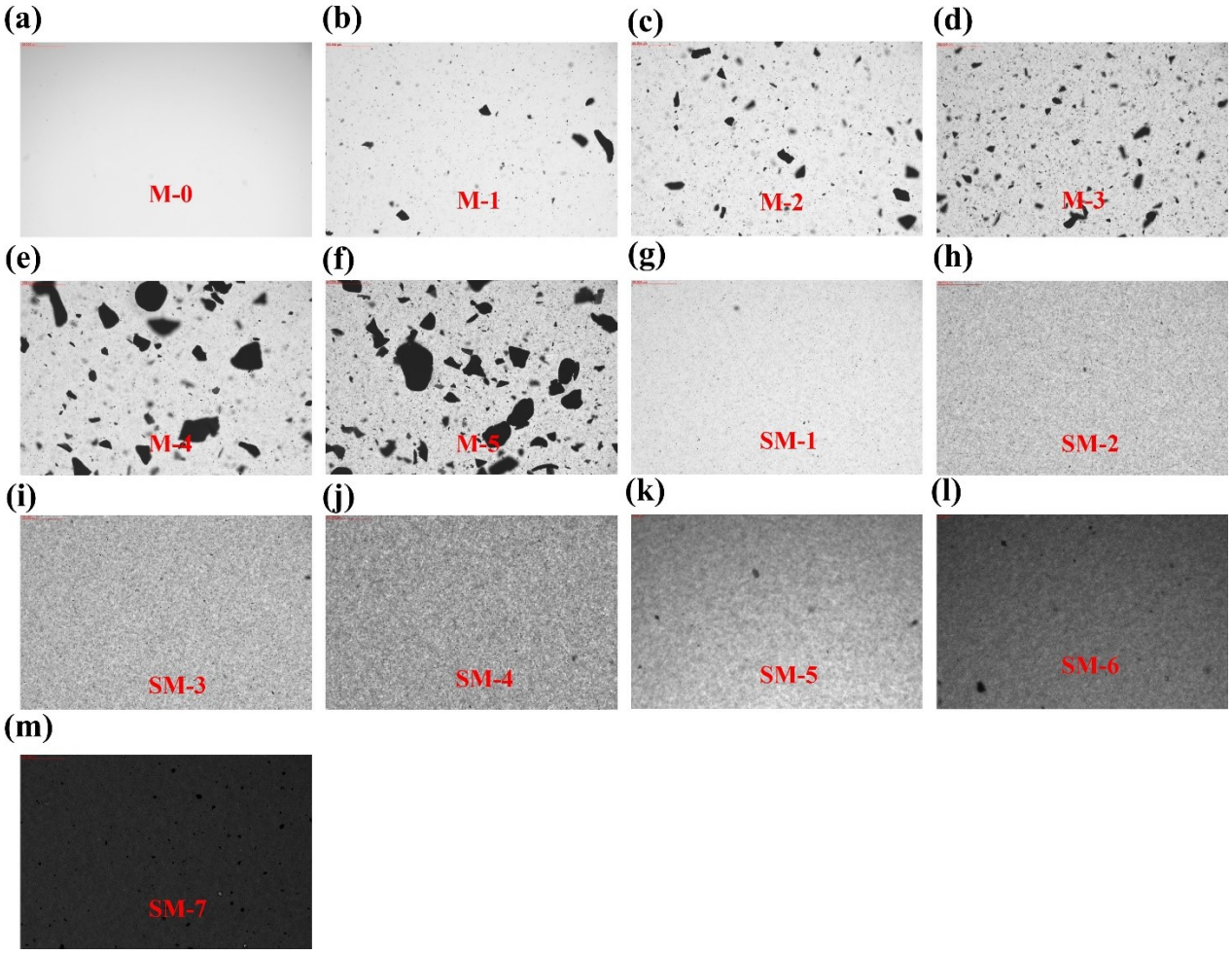

Figure S9. Optical microscope photos of different films.

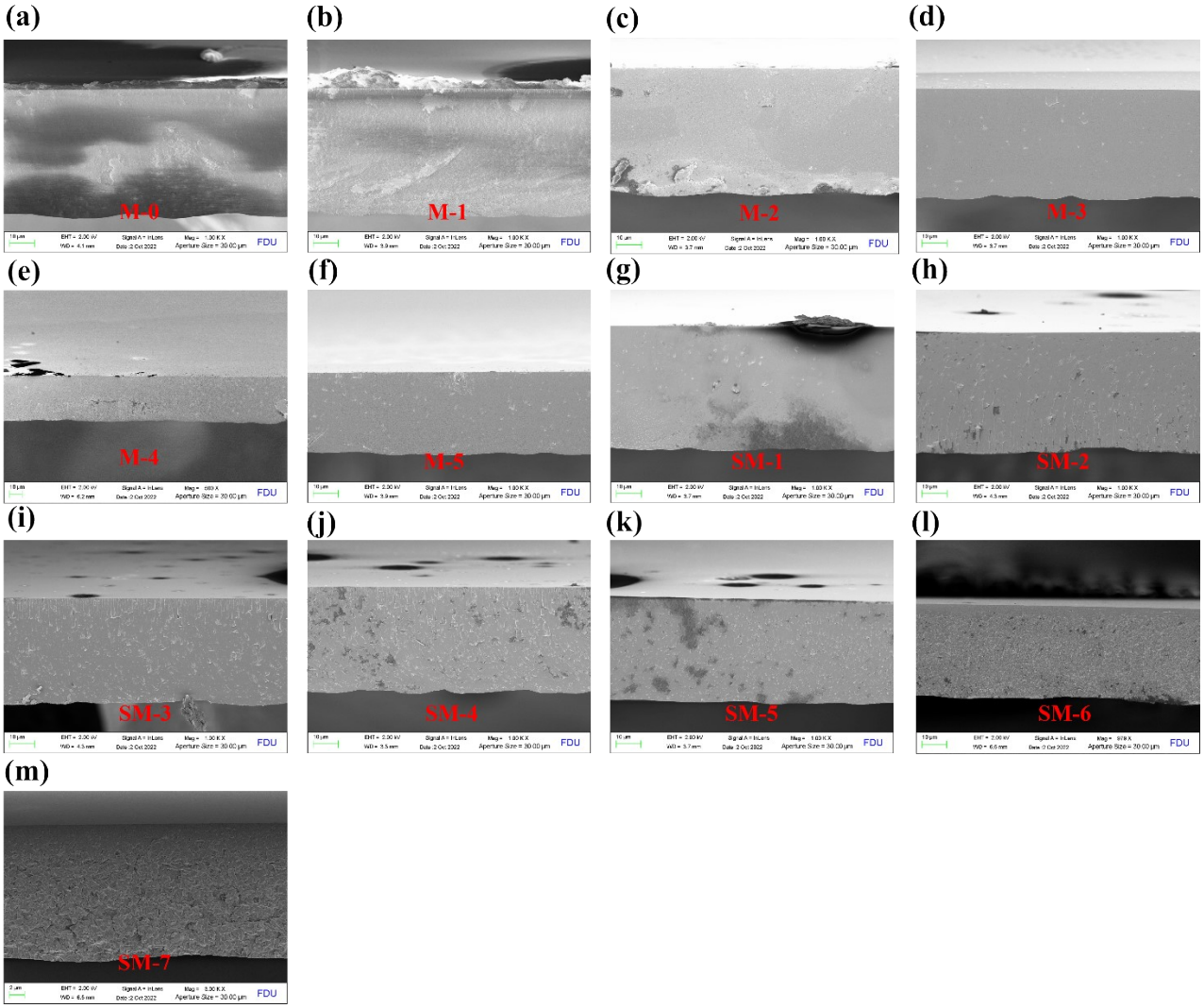

Figure S10. SEM image of cross section of different films.

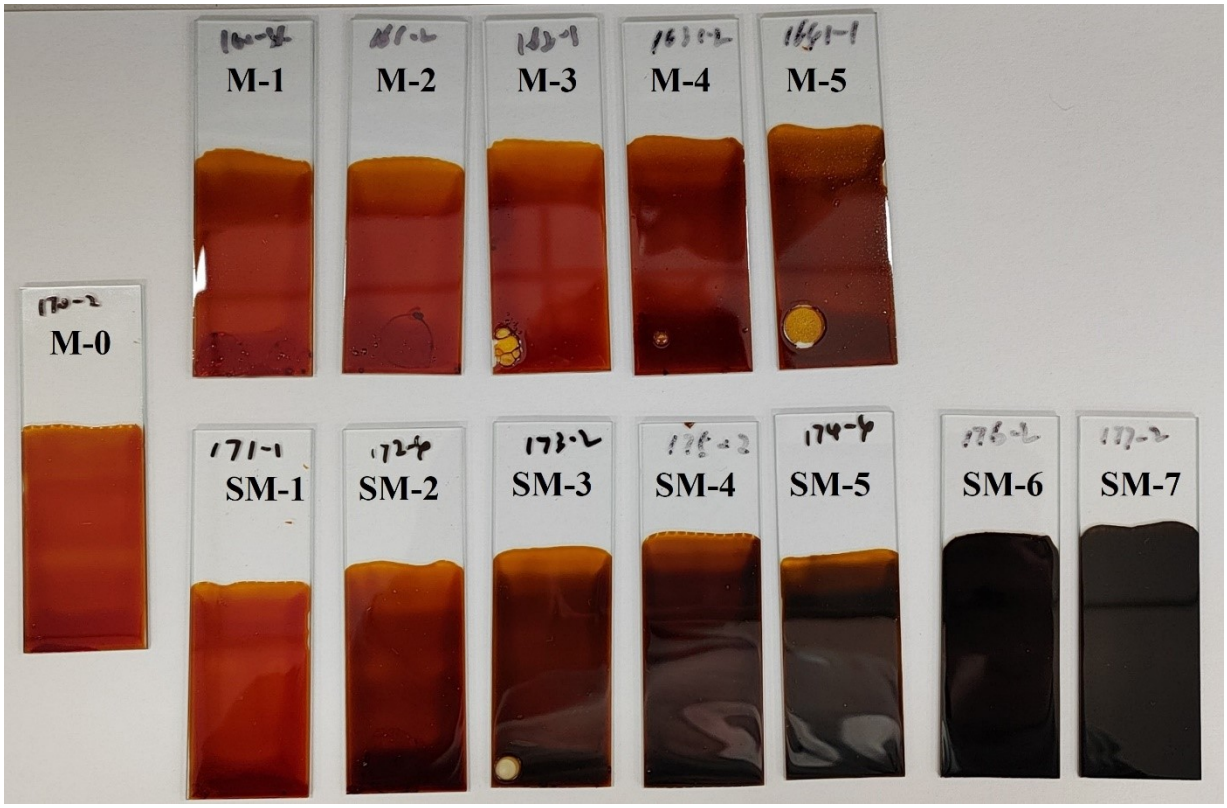

Figure S11. Photograph of different films

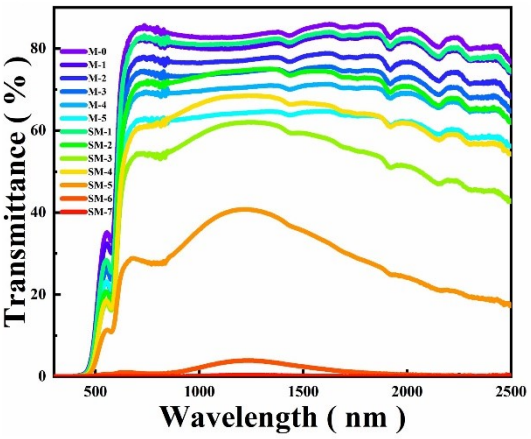

Figure S12. UV–vis transmission spectra of different films.

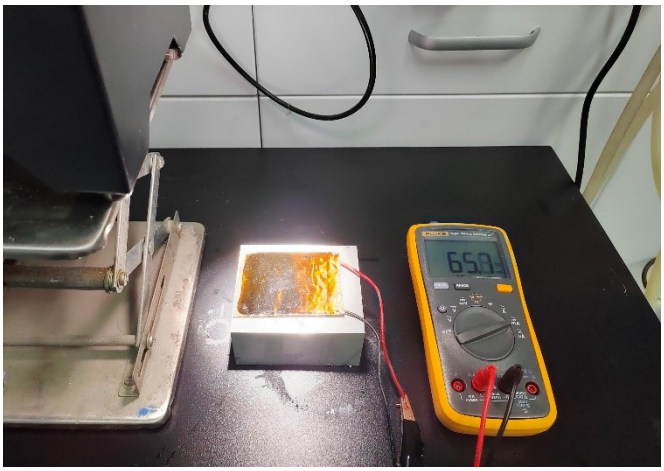

Figure S13. Photograph of the device used in thermoelectric power generation experiment under simulated solar light irradiation.

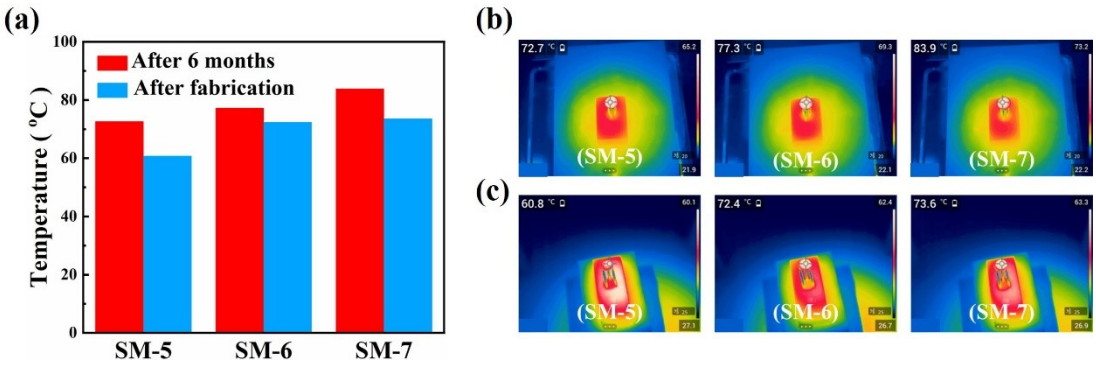

Figure S14. (a) Histogram of surface temperature of different films (SM-5, SM-6, SM-7) after 20 s simulated solar light irradiation at the beginning of preparation and after 6 months. (b) Surface temperature distribution after 20 s simulated solar light irradiation of different films (SM-5, SM-6, SM-7) at the beginning of preparation. (c) Surface temperature distribution after 20 s simulated solar light irradiation of different films (SM-5, SM-6, SM-7) after 6 months.

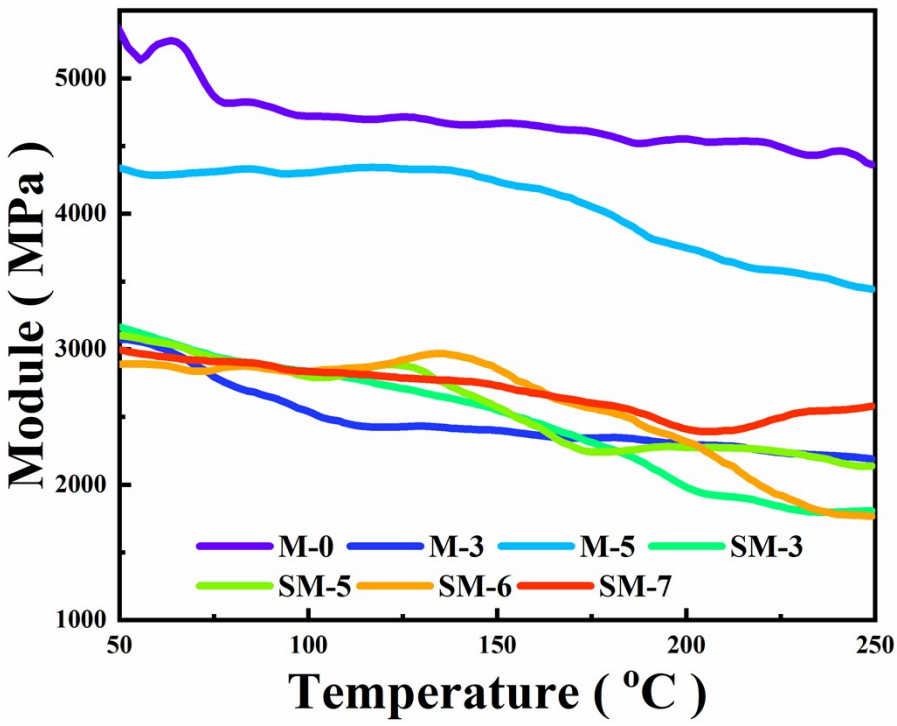

Figure S15. Dynamic mechanical analysis (DMA) curves of various composite films.

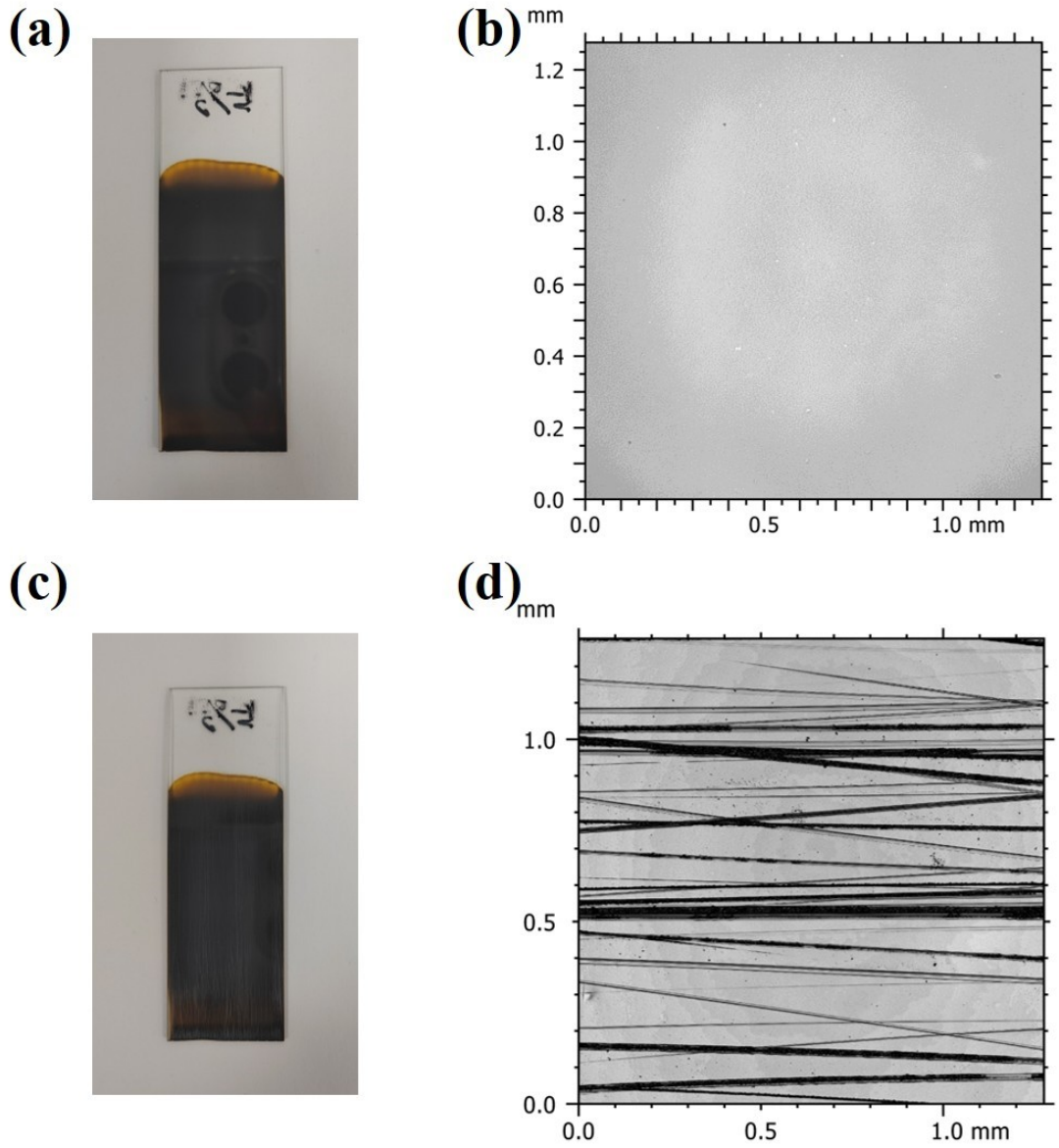

Figure S16. Photograph of film MM-7 (a) before and (c) after friction test; macroscopic image of film MM-7 (b) before and (d) after friction test.